Specifying Air-Sea Exchange Coefficients in the High-Wind Regime of a Mature Tropical Cyclone by an Adjoint Data Assimilation Method

Kosuke Ito, Yoichi Ishikawa, and Toshiyuki Awaji
Department of Geophysics, Kyoto University, Kyoto, Japan

Abstract

Uncertainty in the values of air-sea exchange coefficients has a detrimental effect on tropical cyclone (TC) modeling. Since a TC is one of the most destructive disasters, a method is required to reduce such uncertainty with respect to scientific progress and disaster prevention. In this study, we investigate the feasibility of specifying air-sea exchange coefficients in the high-wind regime of a mature TC by an identical twin experiment using the adjoint data assimilation method. The forward integration is executed by an intermediate cloud-resolving atmosphere-ocean coupled model, while the datasets for the backward integration are sampled as in multiple aircraft missions. Our results show that the air-sea exchange coefficients are successfully improved toward the "True" values. The updated air-sea exchange coefficients yield persistent improvements in the maximum wind speed, the radius of maximum wind, the radius of strong updraft, and in the distribution of water vapor. Without adjustment of the exchange coefficients, the analysis field of the inner-core is contaminated, even if the initial state is modified by the adjoint method.

1. Introduction

It has been proposed that a tropical cyclone (TC) can intensify and maintain its circulation against surface friction through the self-inducement of anomalous fluxes of moist enthalpy from the sea surface. This mechanism is termed "wind-induced surface heat exchange" (WISHE) (Emanuel 1986). According to the WISHE mechanism, the maximum tangential wind speed depends on the ratio of the enthalpy coefficient (C_K) to the drag coefficient (C_D). The radius of maximum wind (RMW) is also thought to depend on the ratio of these coefficients if the outer radius of TC is constant. However, derivation of the surface momentum and enthalpy flux from direct eddy correlation measurements is only reliable for wind speeds up to 30 m s^{-1} in spite of the recent efforts (Black et al. 2007). Powell et al. (2003) showed that the value of C_D should decrease at wind speeds over 30 m s^{-1} by composite analysis of dropsonde observations of wind profile within a "surface layer", which is hard to define accurately. The behavior of C_D was consistent with values derived from the coupled ocean wave and wave boundary model of Moon et al. (2004), though their estimates fall well short of providing quantitative agreement. Even qualitatively, there is no consensus on the behavior of C_K for winds over 30 m s^{-1}. In terms of the estimates of maximum potential intensity based on the WISHE mechanism, the ratio C_K/C_D is thought to be more uncertain than other parameters such as sea surface temperature (SST), outflow temperature, and ambient relative humidity (Montgomery et al. 2006).

An adjoint data assimilation method is one of the powerful candidates of reducing such uncertainty. The basic idea of adjoint calculations is to define a cost function that quantifies the total misfit between the model results and the observations. The adjoint equations effectively transform the misfit into the gradient of the cost function with respect to the control variables suited to the problem. The control variables are determined to minimize the cost function leading to optimal estimates of the model fields. Here, air-sea exchange coefficients, together with the initial state of the assimilation window, are chosen as control variables as in Yu and O'Brien (1991), though the initial state alone is usually employed in operational forecasts. Using this method, observational data outside the boundary layer such as wind velocity, the mixing ratio of water vapor, and ocean mixed layer (ML) momentum, which are relatively accessible compared to the direct eddy correlation measurements within the boundary layer, are assimilated into the model in order to evaluate C_D and C_K values suitable for the actual state through the model physics. This method seems very attractive, but the estimation for air-sea exchange coefficients in a TC has not been explored.

In this paper, the feasibility of the estimation is investigated using a simple atmosphere-ocean coupled model through the re-analysis of the datasets in order to ensure that existing observations are sufficient and that the problem is correctly posed in the sense described by Navon (1998). The possible impact of the estimation on the analysis fields is also investigated. We perform an identical twin experiment as a first step toward realistic estimation with the aim of improving both the dynamical representation of TC events and energy transport along the storm tracks as well as better intensity prediction.

2. Experimental setting

2.1 Numerical model

Our coupled model employs the nonhydrostatic, axisymmetric, cloud-resolving TC model originally written by Rotunno and Emanuel (1987). The version used here includes the implementation of dissipative heating (Bister and Emanuel 1998) and a third-order upwind advection scheme. In brief, the nonhydrostatic, compressible equation of motion is integrated with the prognostic equations for radial velocity u, tangential velocity v, vertical velocity w, potential temperature θ, nondimensional pressure π, and mixing ratios of water vapor q_v, and of liquid water, q_l. We employ the long (short) time step of 2 s (1 s) and an experimental period of 10 days, and describe values of air-sea exchange coefficients and an SST field as shown below. Otherwise, the experimental parameters are the same as those used in '4 × run' of Persing and Montgomery (2003). The domain has 400 × 80 grids with a radial grid spacing of 3.75 km and vertical grid spacing of 312.5 m. The vortex is given at day 0.0 with a maximum tangential wind speed of 12.7 m s^{-1} at a radius r taken as 82.5 km from the center. The SST at day 0.0 is assumed to be 30°C. The SST before the storm passage decreases linearly with time to 27°C on day 10.0, with the latter value used as a boundary condition. This decrease reflects the typical variation in the Northwest Pacific in autumn when a TC travels toward northwest.

We couple a one-dimensional ocean mixed layer (ML) model (Schade and Emanuel 1999) to the TC model. The SST further decreases during the storm passage due to the entrainment of colder water from below, while ML momentum χ is driven by surface stress. A TC is assumed to be translating in a straight line at a constant speed of 6 m s^{-1} over an open ocean with an unperturbed ML depth of 30 m. The ML momentum at day 0.0 is assumed to be zero. The means of coupling is as in Emanuel et al. (2004).

We focus on the water vapor exchange coefficient C_E instead of the enthalpy coefficient C_K, since calculated latent heat fluxes

Corresponding author: Kosuke Ito, Department of Geophysics, Kyoto University, Kitashirakawa-Oiwake-Cho, Sakyo-Ku, Kyoto, Japan. E-mail: itokosk@kugi.kyoto-u.ac.jp.

Table 1. The values of air-sea exchange coefficients used in the "True" and in the "NoAsm" case together with these values obtained from adjoint data assimilation method in the "Asm_Coef" case. Note that the values for low-wind regime are not adjusted in the "Asm_Coef" case as indicated by the values in parentheses.

i	$C_{D,i}$			$C_{E,i}$		
	True	NoAsm	AsmCoef	True	NoAsm	AsmCoef
0	1.14	1.14	(1.14)	1.15	1.15	(1.15)
10	1.14	1.14	(1.14)	1.15	1.15	(1.15)
20	1.79	1.79	1.79	1.20	1.15	1.21
30	2.30	2.44	2.30	1.30	1.15	1.30
40	2.05	2.44	2.08	1.40	1.15	1.39
50	1.50	2.44	1.78	1.50	1.15	1.37
60	1.50	2.44	1.78	1.50	1.15	1.42
70	1.50	2.44	0.97	1.50	1.15	1.43

are more than an order of magnitude greater than sensible heat fluxes. For simplicity, the C_D and C_E values are assumed to be functions of the wind speed at the lowest layer of the atmospheric model (z = 156.25 m) as a zero-th order approximation. The behavior is determined by the discrete values at 10 m s^{-1} intervals ($C_{D,i}$ and $C_{E,i}$; surface wind speed index i = 0, 10, 20, …) in conjunction with the linear interpolation whose weight is α_i (r, t) ($0 \le \alpha_i \le 1$; the variable t represents time).

2.2 Identical twin experiment

In our identical twin experiment, the "True" field is generated by numerical integration of the coupled model, while another run is performed with the same setting except for random errors in the initial state of the assimilation window and the "wrong" coefficients in high-wind regimes ($i \ge 20$ m s^{-1}). The result of the latter case is referred to as the "NoAsm" field. Here, the pseudo observations are generated by adding Gaussian noise to variables in the "True" field. The analysis field is generated by digesting the observations with an adjoint data assimilation method. In an experiment termed "Asm_Coef", the control variables are the $C_{D,i}$ and $C_{E,i}$ values together with the initial state settings. In order to evaluate the impact of the estimates of C_D and C_E, we also perform an "Asm_NoCoef" experiment in which the initial state settings alone are taken as the control variables. We employ a relatively long assimilation window from day 6.0 to day 10.0, in which the uncertainty in the values of C_D and C_E influences the results much more than those in case of a shorter assimilation window.

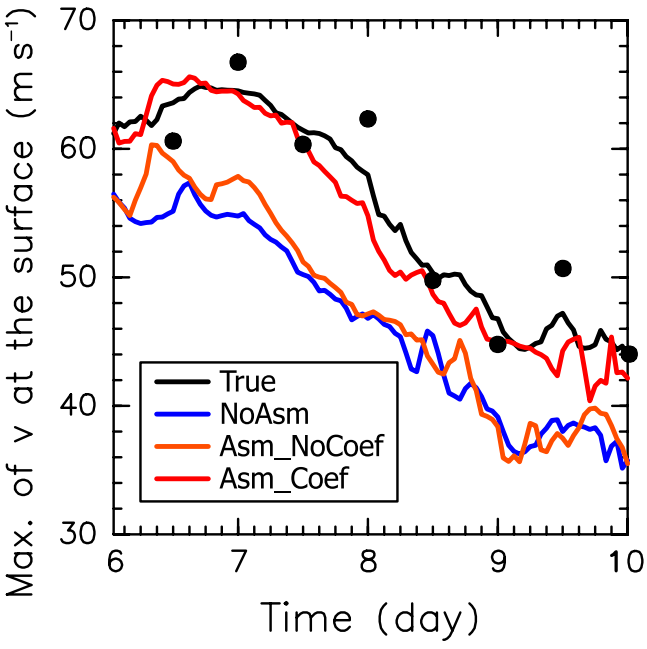

Fig. 1. Time series of the maximum tangential wind velocity at the lowest layer of the atmospheric model. Closed circles denote the observed values.

The behavior of the $C_{D,i}$ for the high-wind regime used to generate the "True" field mimics the values obtained by the recent composite analysis of the observations (Powell et al. 2003). The values in the range over 50 m s^{-1} are assumed to be same as those at 50 m s^{-1}. We assign the values of C_E for the high-wind condition so that the ratio $C_{E,i}/C_{D,i}$ approaches to unity in the extreme condition. For the "NoAsm" run, we mimic the values given in Large and Pond (1981), which are commonly used bulk formulae. The values are constant over 30 m s^{-1}. These coefficients are summarized in Table 1. Random errors in the initial state are generated by using the background error covariance matrix **B** described below.

For the "Asm_Coef" run, the cost function J is defined as follows:

$$J \equiv \frac{1}{2}(\mathbf{x}_0 - \mathbf{x}_b)^{\mathrm{T}}\mathbf{B}^{-1}(\mathbf{x}_0 - \mathbf{x}_b) + \sum_t \frac{1}{2}(\mathbf{H}\mathbf{x} - \mathbf{y})^{\mathrm{T}}\mathbf{R}^{-1}(\mathbf{H}\mathbf{x} - \mathbf{y}) + \sum_i \sum_r \sum_t \alpha_i (F_{C_{D,i}} + F_{C_{E,i}}), \quad (1)$$

where $\mathbf{x}$ is the prognostic variable vector, $\mathbf{x}_0$ represents the initial condition, $\mathbf{y}$ represents the observation field, $\mathbf{H}$ is the observational operator, and the subscript b denotes the background value taken from "NoAsm" experiment. The values of $F_{C_{D,i}}$ and $F_{C_{E,i}}$ are equal to $(1/2)K_{C_{D,i}}(C_{D,i} - (C_{D,i})_b)^2$ and $(1/2)K_{C_{E,i}}(C_{E,i} - (C_{E,i})_b)^2$, respectively, where the coefficients $K_{C_{D,i}}$ and $K_{C_{E,i}}$ are the Gauss precision moduli. The matrix **R** is the observation error covariance matrix. The second term on the rhs represents the data misfit, while the others measure the distance from the background field. We prescribe **B** using a Gaussian function that decays with the e-folding scale of the influential radii. The latter is given as one-fourth of the typical wavelength indicated by two-dimensional Fourier analysis of the perturbed "True" fields at day 6.0. The magnitudes are given as the sample variance of the "True" run from day 4.0 to day 8.0. For simplicity, only the background error covariance of the same variable is used. The diagonal elements of **R** are assigned to be 0.05 times those of **B**, while the non-diagonal elements of **R** are assumed to be zero.

The data misfit is transformed into the gradient of the cost function by backward integration of the adjoint equation with the aid of the adjoint variables $\lambda(\mathbf{x})$. The code for the adjoint equation is obtained using the Tangent linear and Adjoint Model Compiler (TAMC) (Giering and Kaminski 1998). The model physics used in the adjoint system is slightly different from that used in the forward model. For example, the terms associated with sound waves and microphysics are excluded. The gradients with respect to $C_{D,i}$ and $C_{E,i}$ are calculated as follows (see Yu and O'Brien (1991) for a derivation):

$$\frac{\partial J}{\partial C_{D,i}} = \sum_r \sum_t \alpha_i \left\{ |\mathbf{V}_s|(\mathbf{V}_s \cdot \lambda(\mathbf{V}_s)) + |\mathbf{V}_s|^2 \lambda(\chi) + \frac{\partial F_{C_{D,i}}}{\partial C_{D,i}} \right\}, \quad (2)$$

$$\frac{\partial J}{\partial C_{E,i}} = \sum_r \sum_t \alpha_i \left\{ |\mathbf{V}_s|(q_{v_s} - q^*_{v_s})\lambda(q_{v_s}) + \frac{\partial F_{C_{E,i}}}{\partial C_{E,i}} \right\}, \quad (3)$$

where the subscript s represents the corresponding value at the sea surface, and $q^*_{v_s}$ is the saturation mixing ratio of water vapor with $\mathbf{V}_s \equiv (u_s, v_s)$ and $\lambda(\mathbf{V}_s) \equiv (\lambda(u_s), \lambda(v_s))$. The first and the second term on the rhs in equation (2) corresponds to the contribution of surface friction on $\mathbf{V}_s$ and χ, respectively. The first term on the rhs in equation (3) corresponds to the contribution of evaporation at the sea surface. The updates of C_D and C_E are obtained using the steepest descent method.

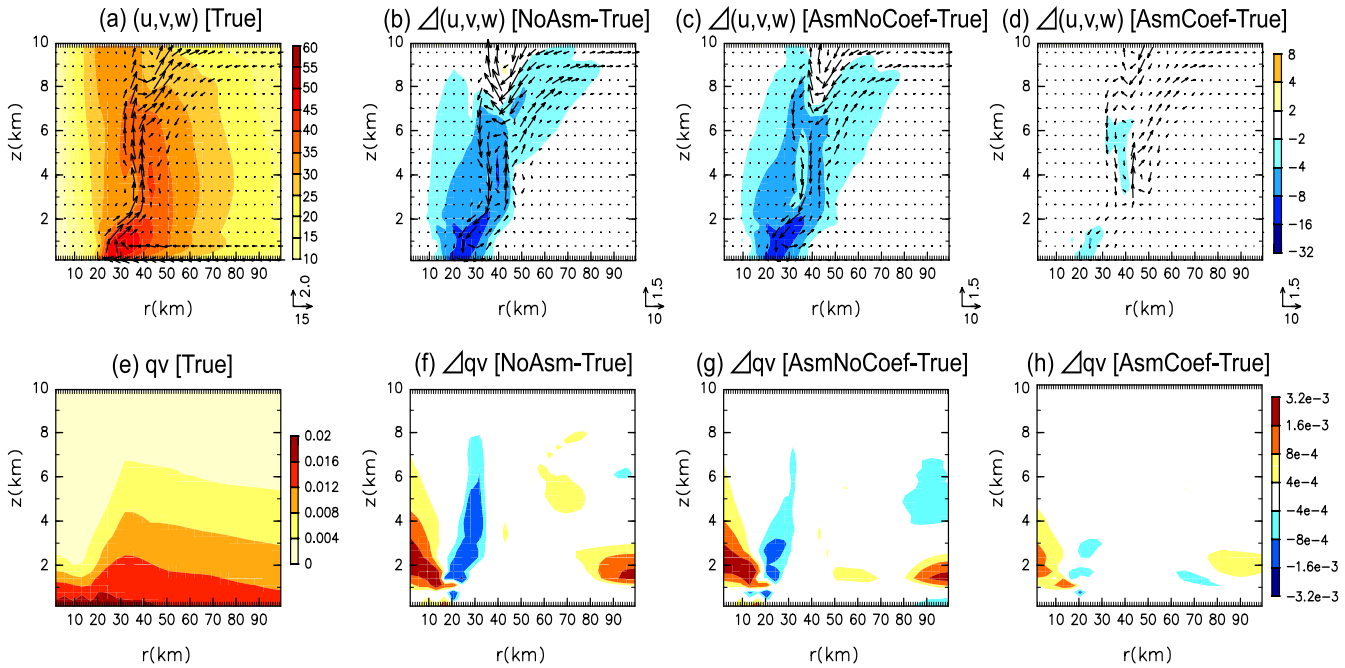

Fig. 2. Radius-height time mean structure from day 9.0 to day 10.0: [Panel (a)] tangential velocity v (contours), radial velocity u and vertical velocity w (vectors) from the "True" run. [Panels (b)–(d)] Errors in "NoAsm", "Asm_NoCoef" and "Asm_Coef" fields are denoted, respectively. Unit vectors are shown in the bottom of the rhs of each panel. [Panels (e)–(h)] same as in the panels (a)–(d) but for the q_v (contours).

We assume that the data are sampled every 12 hours at each grid point below 5 km within a radius of 150 km from the storm center, as in multiple aircraft missions (e.g., Montgomery et al. 2006; Black et al. 2007). The observed variables are u, v, q_v, and χ. Note that mass streamfunction of the secondary flow is selected as a control variable instead of u and w to preclude the dominant sound wave component, and that an artificial dumping effect proportional to the wind speed is introduced into the adjoint equation to ensure completion of the numerical calculation.

3. Results

3.1 Estimates of C_D and C_E

Table 1 shows the estimated C_D and C_E values in the "Asm_Coef" case together with those used in the "True" and "NoAsm" experiments. The C_D and C_E used in the "NoAsm" experiment are successfully improved toward the "True" coefficients via the adjoint data assimilation method. The intake of the observations at intervals of 12 hours over 4 days is sufficient to provide a rough estimate. As a result, the ratio C_E/C_D is correctly increased toward the "True" values. The estimate is essentially unaffected by the ill-posedness of the problem such as nonuniqueness and instability of parameters (Navon 1998).

It is worth emphasizing that this improvement is obtained without taking into account microphysical processes for backward integration. More specifically, the considerable improvement in the value of the $C_{E,i}$ obtained in the present system is achieved by using information on the excess/paucity of q_v through advection and diffusion processes. This fact seems to support our estimate as relevant to a real TC because fast growing fluctuations associated with microphysical processes threaten the numerical stability of the backward integration in longer assimilation windows suitable for the estimation of model parameters. However, the relatively inaccurate estimation of the coefficients for wind speeds over 40 m s^{-1} may partly result from the fact that we neglect the microphysical processes for backward integration.

3.2 Potential impact on intensity and structure

To investigate the potential impact of the adjusted coefficients on the improvement of the intensity, we assess the time series of the maximum tangential wind speed at the surface during the assimilation window (Fig. 1). The values in the "True" field range from 64.9 m s^{-1} (day 6.7) to 43.7 m s^{-1} (day 10.0), respectively. The decay of the vortex during the latter half reflects the decrease of SST before the storm passage, and it depends slightly on the ratio of C_E/C_D. In the "Asm_NoCoef" experiment, the modified surface wind at the initial state is locally adjusted by the stronger surface friction very rapidly. This fact suggests that the "wrong" C_D has an adverse effect on the maximum surface wind speed in the analysis field. The TC vortex is stronger than the "NoAsm" case during the first half of the assimilation period thanks to a spurious positive anomaly of water vapor at the initial state which compensates for the smaller C_E (figures not shown). However, it is likely that part of the improvement may be an artifact of the initial vortex adjustment associated with the adjoint data assimilation method. In the latter half period, persistent errors in C_D and C_E contaminate the analysis field in the "Asm_NoCoef" experiment. The errors in "Asm_Coef" case are far smaller compared to other cases. This means that updates of C_D and C_E in high-wind regimes are effective in controlling the analysis field on a longer time scale. The stronger vortex in the "Asm_Coef" experiment is consistent with increase in the C_E/C_D ratio according to the WISHE mechanism.

Figure 2a shows that the time mean "True" wind fields from day 9.0 to day 10.0 capture the fundamental characteristics of the TC. The motion component, v, is characterized by a sharp maximum, whereas the u field shows inward (outward) flow in the boundary layer (upper troposphere). The vertical velocity w indicates the formation of the eyewall encircling the eye. Based on Fig. 2a, the error fields in the "NoAsm", "Asm_NoCoef", and "Asm_Coef" cases clearly illustrate the potential impact of the adjusted C_D and C_E (Figs. 2b, 2c, and 2d). As seen in Fig. 1, the TC vortex is weakly simulated in the "NoAsm" and "Asm_NoCoef" cases. The maximum errors in these cases are observed inside the "True" eyewall region, which means that the RMW is located outside the "True" region. The error fields of u and

w along the eyewall in the lower troposphere indicate that the radius of the strong updraft is also located outside. In contrast, the velocity fields are much improved in the "Asm_Coef" case. For example, the intensity of the TC is persistently modified, as in the RMW and the radius of the strong draft. The improvements in the intensity and RMW are consistent with the mechanism of WISHE.

The errors in the intensity can be explained by considering the distributions of q_v besides the frictional force exerted locally at the surface. Figure 2e shows time-averaged q_v in the "True" case from day 9.0 to day 10.0. Figures 2f, 2g, and 2h show the errors in "NoAsm", "Asm_NoCoef", and "Asm_Coef" cases. A deficit in q_v is seen along the eyewall region of the middle troposphere in the "Asm_NoCoef" experiment, and suggests that improvement of the initial state is unlikely to provide full diabatic energization on a longer time scale. This reflects the fact that a parcel in the eyewall updraft travels from the surface to the middle troposphere over a time scale of less than one day (Persing and Montgomery 2003). That is, inflow at the surface after day 7.0 or so is contaminated by the errors of C_E values. In the "Asm_Coef" case, the distribution of q_v is considerably improved by the removal of the persistent error source at the surface.

4. Summary and discussion

The feasibility of estimating the drag coefficient (C_D) and the water vapor exchange coefficient (C_E) in the high-wind regime of a tropical cyclone (TC) through the adjoint data assimilation method is investigated. We employ an intermediate cloud-resolving atmosphere-ocean coupled model and perform an identical twin experiment. We confirm the feasibility of the estimation in the light of the model physics for a mature TC. As the quantity of campaign observations is sufficient to improve both C_D and C_E toward their "True" values, the adjusted C_D and C_E terms yield substantial improvements in the intensity and in the radius of maximum winds. These improvements are consistent with the mechanism of wind-induced surface heat exchange.

The improvement resulting from the modified initial state may endure longer than in the present system if we introduce the interaction between the large scale flow and a TC by using a sophisticated three-dimensional model. Nevertheless, it is expected that persistent errors will contaminate the analysis fields, especially in the TC inner-core dynamics, unless the values of the C_D and C_E are amended.

The study shows an encouraging result for improving the TC prediction by adjusting the momentum and enthalpy fluxes through an adjoint data assimilation method. However, the limitation arising from simplified model physics must be recognized for practical use. In fact, our model does not capture vortex Rossby waves and ice phase processes, which may affect the TC intensity and structure. Moreover, further progress requires better physical representation of C_D and C_E. The dependencies of C_D and C_E on atmospheric stability and sea state as well as surface wind speeds should be investigated for a better physical representation. Nevertheless, our study shows the potential impact of adjusted air-sea exchange coefficients in improving TC intensity and structure.

Acknowledgments

We specially thank Dr. K. Emanuel who generously provided the forward model and Dr. T. Takemi, Dr. S. Otsuka and Mr. Y. Miyamoto for providing useful comments. Thanks are extended to Dr. J. Matthews for reading manuscript. The present work is partly supported by Grant-in-Aid for JSPS Fellows.

References

Bister, M., and K. Emanuel, 1998: Dissipative heating and hurricane intensity. *Meteor. Atmos. Phys.*, **65**, 233−240.

Black, P., E. D'Asaro, W. Drennan, J. French, P. Niiler, T. Sanford, E. Terrill, E. Walsh, and J. Zhang, 2007: Air−sea exchange in hurricanes: Synthesis of observations from the coupled boundary layer air−sea transfer experiment. *Bull. Amer. Meteor. Soc.*, **88**, 357−374.

Emanuel, K., 1986: An air-sea interaction theory for tropical cyclones. Part I: Steady-state maintenance. *J. Atmos. Sci.*, **43**, 585−605.

Emanuel, K., C. DesAutels, C. Holloway, and R. Korty, 2004: Environmental control of tropical cyclone intensity. *J. Atmos. Sci.*, **61**, 843−858.

Giering, R., and T. Kaminski, 1998: Recipes for adjoint code construction. *ACM Transactions on Mathematical Software*, **24**, 437−474.

Montgomery, M., M. Bell, S. Aberson, and M. Black, 2006: Hurricane Isabel (2003): New insights into the physics of intense storms. Part I: Mean vortex structure and maximum intensity estimates. *Bull. Amer. Meteor. Soc.*, **87**, 1335−1347.

Moon, I., I. Ginis, and T. Hara, 2004: Effect of surface waves on air−sea momentum exchange. Part II: Behavior of drag coefficient under tropical cyclones. *J. Atmos. Sci.*, **61**, 2334−2348.

Navon, I., 1998: Practical and theoretical aspects of adjoint parameter estimation and identifiability in meteorology and oceanography. *Dyn. Atmos. Ocean.*, **27**, 55−79.

Persing, J., and M. Montgomery, 2003: Hurricane superintensity. *J. Atmos. Sci.*, **60**, 2349−2371.

Powell, M., P. Vickery, and T. Reinhold, 2003: Reduced drag coefficient for high wind speeds in tropical cyclones. *Nature*, **422**, 279−283.

Rotunno, R., and K. Emanuel, 1987: An air−sea interaction theory for tropical cyclones. Part II: Evolutionary study using a nonhydrostatic axisymmetric numerical model. *J. Atmos. Sci.*, **44**, 542−561.

Schade, L., and K. Emanuel, 1999: The ocean's effect on the intensity of tropical cyclones: Results from a simple coupled atmosphere−ocean model. *J. Atmos. Sci.*, **56**, 642−651.

Yu, L., and J. O'Brien, 1991: Variational estimation of the wind stress drag coefficient and the oceanic eddy viscosity profile. *J. Phys. Oceanogr.*, **21**, 709−719.

Manuscript received 13 November 2009, *accepted 7 January 2010*
SOLA: *http://www.jstage.jst.go.jp/browse/sola/*